Neurobiology of Disease 121 (2019) 34–46

Contents lists available at ScienceDirect

Neurobiology of Disease

journal homepage: www.elsevier.com/locate/ynbdi

The *PPARGC1A* locus and CNS-specific PGC-1α isoforms are associated with Parkinson's Disease

Selma M. Soyal[a,*,1], Greta Zara[a,1], Boris Ferger[b], Thomas K. Felder[c], Markus Kwik[a], Charity Nofziger[a], Silvia Dossena[a], Christine Schwienbacher[d], Andrew A. Hicks[d], Peter P. Pramstaller[d], Markus Paulmichl[e], Serge Weis[f], Wolfgang Patsch[a,*]

[a] Institute of Pharmacology and Toxicology, Paracelsus Medical University, Salzburg, Austria
[b] Boehringer Ingelheim Pharma GmbH & Co. KG, Biberachan der Riss, Germany
[c] Department of Laboratory Medicine, Paracelsus Medical University, Salzburg, Austria
[d] Institute for Biomedicine, Eurac Research, Affiliated Institute of the University of Lübeck, Bolzano, Italy
[e] Center for Health & Bioresources, Austrian Institute of Technology, Vienna, Austria
[f] Division of Neuropathology, Johannes Kepler University Hospital, Linz, Austria

ARTICLE INFO

Keywords:
Parkinson's disease
Lewy body dementia
PPARGC1A
PGC-1α
haplotypes

ABSTRACT

Parkinson's disease (PD) is the second most common neurodegenerative disease worldwide. PGC-1α, encoded by *PPARGC1A*, is a transcriptional co-activator that has been implicated in the pathogenesis of neurodegenerative disorders. We recently discovered multiple new *PPARGC1A* transcripts that initiate from a novel promoter located far upstream of the reference gene promoter, are CNS-specific and are more abundant than reference gene transcripts in whole brain. These CNS-specific transcripts encode two main full-length and several truncated isoforms *via* alternative splicing. Truncated CNS-isoforms include 17 kDa proteins that lack the second LXXLL motif serving as an interaction site for several nuclear receptors. We now determined expression levels of CNS- and reference gene transcripts in 5 brain regions of 21, 8, and 13 deceased subjects with idiopathic PD, Lewy body dementia and controls without neurodegenerative disorders, respectively. We observed reductions of CNS-specific transcripts (encoding full-length isoforms) only in the substantia nigra pars compacta of PD and Lewy body dementia. However, in the substantia nigra and globus pallidus of PD cases we found an up-regulation of transcripts encoding the 17 kDa proteins that inhibited the co-activation of several transcription factors by full-length PGC-1α proteins in transfection assays. In two established animal models of PD, the *PPARGC1A* expression profiles differed from the profile in human PD in that the levels of CNS- and reference gene transcripts were decreased in several brain regions. Furthermore, we identified haplotypes in the CNS-specific region of *PPARGC1A* that appeared protective for PD in a clinical cohort and a post-mortem sample ($P = .0002$). Thus, functional and genetic studies support a role of the CNS-specific *PPARGC1A* locus in PD.

1. Introduction

Second to Alzheimer's disease (AD), Parkinson's disease (PD) is the most common neurodegenerative disorder worldwide. As PD risk increases with age, the incidence of this devastating and debilitating condition is predicted to have increased a further 50% by 2030 (Dorsey et al., 2007; Tanner and Goldman, 1996). Clinically, PD is characterized by classical motor deficits that result from loss of dopaminergic neurons in the substantia nigra (SN) pars compacta (SNPC). A range of other symptoms that occur in the course of PD reflects disturbances in other brain regions and/or neurotransmitter systems (Kalia and Lang, 2015). Furthermore, the incidence of dementia in PD is several-fold higher than in age-matched controls (Hely et al., 2008). Apart from the loss of dopaminergic neurons in the SNPC, alpha-synuclein pathology is the neuropathological hallmark of PD. It consists of proteinaceous inclusions enriched in filamentous forms of α-synuclein and other proteins in the cell bodies (Lewy bodies) and processes of neurons (Lewy neurites) (Abeliovich and Gitler, 2016; Spillantini et al., 1997). Clues about the

Abbreviations: AD, Alzheimer's disease; LBD, Lewy body dementia; MPTP, 1-methyl-4-phenyl-1,2,3,6-tetrahydropyridine; PD, Parkinson's disease; PGC-1α, peroxisome proliferator activated receptor gamma coactivator 1 alpha; RG, reference gene; SNP, single nucleotide polymorphism; SNPC, substantia nigra pars compacta

* Corresponding authors at: Institute of Pharmacology and Toxicology, Paracelsus Medical University, Strubergasse 21, 5020 Salzburg, Austria.
E-mail addresses: selma.soyal@pmu.ac.at (S.M. Soyal), wolfgang.patsch@pmu.ac.at (W. Patsch).

[1] These authors contributed equally to this work.

https://doi.org/10.1016/j.nbd.2018.09.016
Received 10 March 2018; Received in revised form 14 July 2018; Accepted 14 September 2018
Available online 17 September 2018

etiology of PD have been garnered *via* pathological, genetic and epidemiological studies and several environmental and genetic risk factors have been identified (Abeliovich and Gitler, 2016; Kalia and Lang, 2015). Converging genetic evidence supports defects in endosomal trafficking, protein disposal *via* the proteasome and/or lysosome-autophagy system and mitochondrial function (International Parkinson Disease Genomics et al., 2011; Nalls et al., 2014).

Like PD, Lewy body dementia (LBD) is characterized by Lewy body pathology in limbic and cortical structures. However, progressive cognitive impairment, visual hallucinations and fluctuations of attention occur prior to or within one year of Parkinsonian motor symptoms in LBD, while the interval between motor symptoms and cognitive impairment is typically much longer in PD dementia (McKeith et al., 2005).

Peroxisome proliferator activated receptor gamma coactivator 1α (PGC-1α), encoded by *PPARGC1A*, is a transcriptional co-activator that integrates transcriptional programs that are relevant in the pathogenesis of neurodegenerative disorders and include mitochondrial biogenesis and function, the defense against reactive oxygen species and autophagy (Handschin and Spiegelman, 2006; Lin et al., 2005; Lin and Beal, 2006; Soyal et al., 2006; Tsunemi et al., 2012). Indeed, associations of the *PPARGC1A* locus with Huntington disease and amyotrophic lateral sclerosis have been reported previously (Eschbach et al., 2013; Soyal et al., 2012; Weydt et al., 2009). The first indication for a role of PGC-1α in PD came from studies in PGC-1α knock-out mice that demonstrated enhanced sensitivity to the oxidative stressor 1-methyl-4-phenyl-1,2,3,6-tetrahydropyridine (MPTP) (St-Pierre et al., 2006). MPTP-induced degeneration of dopaminergic neurons was prevented by PGC-1α (Mudo et al., 2012). Furthermore, silencing of PGC-1α increased the susceptibility of SH-SY5Y cells to *N*-methyl-4-phenylpyridinium ions and inhibited mitochondrial function (Ye et al., 2017) Overexpression of PGC-1α prevented cell death of embryonic rat midbrain cells transduced with A53T α-synuclein–encoding adenovirus (Zheng et al., 2010). Moreover, progressive Parkinsonism was observed in mice with conditional disruption of the PGC-1α target gene *TFAM* (Ekstrand et al., 2007). In 3D5 cells conditionally overexpressing α-synuclein, knockdown of PGC-1α increased α-synuclein oligomers/aggregates and decreased levels of AKT, GSK3β and p53 (Ebrahim et al., 2010) and α-synuclein toxicity can be reduced by pharmacological activation or overexpression of PGC-1α (Eschbach et al., 2015). In addition, α-synuclein was shown to bind to the PGC-1α promoter in brain tissue and reduced promoter activity of PGC-1α and its target gene expression *in vitro* (Siddiqui et al., 2012).

We recently discovered multiple new *PPARGC1A* transcripts that initiate from a novel promoter located 587 kb upstream of exon 2 (Soyal et al., 2012). We showed that these new transcripts are CNS-specific, are more abundant than the reference gene (RG) transcripts in whole brain and are partially conserved in rodents. Two main transcripts with independent methionine start codons encode full-length CNS-isoforms that differ only at their N-termini from PGC-1α encoded by the RG. Truncated isoforms containing these N-termini exist that are similar to NT-PGC-1α (Zhang et al., 2009) or are encoded by transcripts harboring a stop codon in an extended exon 3 resulting in 17 kDa proteins. The new CNS-promoter lies in a haplotype block clearly separated from the RG promoter, is active in SH-SY5Y and NTERA-2 cl.D1 (NT2/D1) cells and is located within a CpG island. The structure of the CNS transcripts, their CNS-specific expression and their higher expression levels in comparison to RG transcripts has now been confirmed in independent studies (Jiang et al., 2016; Wang et al., 2016).

In most previous studies on PGC-1α and PD, only the RG (Esterbauer et al., 1999) (GenBank NM_013261.3) was addressed and very little is known about the more abundant CNS-specific transcripts/isoforms. We therefore determined levels of various transcripts and proteins encoded by the *PPARGC1A* locus in several regions of post-mortem brain tissues from neuro-pathologically verified PD and LBD cases and controls. Similar measurements were also made in animal models of PD. Furthermore, the CNS-specific *PPARGC1A* genomic region was interrogated for possible associations with PD.

2. Materials and methods

2.1. Post-mortem human resources

Human brain tissue and DNA samples were procured from the brain bank of the Department of Neuropathology, Kepler University Hospital, Linz, Austria. Following federal law, post-mortem tissue can be removed by autopsy for diagnostic or scientific purposes. Upon removal, the brain was separated into the two hemispheres by a mid-sagittal cut which also allows hemi-dissection of the cerebellum and the brain stem. One half of the brain was immediately fixed in 4% formaldehyde for one week prior to neuropathological dissection. The second half of the brain was fresh frozen at −80 °C as follows: The brainstem with the cerebellum was dissected at the level of the pons and midbrain. A slice containing the substantia nigra and nucleus ruber was generated and frozen. The cerebellum was removed from the brainstem by a cut though the cerebellar peduncles. The brainstem was cut into thin slabs perpendicular to its main axis. Slices of the cerebellum were generated parallel to the vermis. The cerebral hemisphere was cut into 1 cm thick coronal slabs and frozen. After thorough gross-anatomical examination of the fixed hemisphere, 20 tissue blocks were cut for histopathological examination. For each block the following staining was performed: Hematoxylin and eosin, Luxol Fast Blue, immunohistochemistry for beta A4 amyloid, tau, phosphorylated tau, tau 3 repeat, tau 4 repeat, α-synuclein, ubiquitin, p62, TDP-43 and FUS. PD related pathology was graded according to Braak et al. in stages 1–6, *i.e.* medulla oblongata (stage 1), medulla oblongata and pontine tegmentum (stage 2), midbrain (stage 3), basal prosencephalon and mesocortex (stage 4), high order sensory association areas of the neocortex (stage 5) and first order sensory association areas of the neocortex (stage 6) (Braak et al., 2003). For LBD, the lesions were typed according to the following criteria: brainstem predominant (type 1), limbic transitional (type 2) and diffuse neocortical (type 3) (McKeith et al., 2005). All examined cases were of the diffuse neocortical type. The topographical localization of neurofibrillary tangles was staged according to Braak & Braak E: transentorhinal cortex (stage I-II), limbic (stage III-IV) and isocortical (stage V-VI) (Braak and Braak, 1991).

Frozen tissue samples were removed with a special trepan (diameter 4 mm) from the frontal lobe, SNPC, globus pallidus, parietal lobe and cerebellum of 21 and 8 deceased subjects with idiopathic PD and LBD, respectively. Tissue samples from 13 subjects who died after age 50 without neurodegenerative disorders with the exception of minor AD neuropathology, but no signs of clinical AD served as controls (Table 1). In addition, DNA samples from 169, 85 and 134 deceased subjects without neurodegenerative disorders, with PD or with AD, respectively, were used for genotyping.

Table 1
Characteristics of post-mortem cases and controls.

Variable	Control	PD	LBD	*P*
Sex, m/f	8/5	16/5	4/4	n.s.
Age of death	76 (11)	80 (7)	80 (7)	n.s.
Post-mortem time, hrs	22 (20)	32 (20)	36 (38)	n.s.
Braak α-synuclein stages (0/1–2/3–4/5–6)	13/0/0/0	0/0/12/9	0/0/0/8	n.d.
Braak tau stages (0/I-II/III-IV/V-VI)	2/8/3/0	1/10/7/3	2/4/2/0	n.s.

PD, Parkinson's disease; LBD, Lewy body dementia; n.s., not significant; n.d., not determined.

2.2. Clinical resources

DNA from 196 subjects with PD and 206 subjects without neurodegenerative disorders from the Genetic Epidemiology in South Tyrolean Studies of Parkinson's disease (GESSPARK) and Dyskinesia, Impulse control and Sleep in Parkinson's disease (DISP) studies were provided by the Neurology department at the Bolzano Central Hospital in collaboration with the Eurac Research Institute for Biomedicine in Bolzano, Italy. All patients and controls were enrolled in the studies conducted through the PD outpatient clinic of the Neurology department following detailed examination by a neurologist. Study-specific questionnaires were filled in following examinations and blood was drawn for biobanking and DNA extraction. In addition, DNA samples from 584 subjects from participants of the Salzburg Atherosclerosis Prevention Program in Subjects at High Individual Risk (SAPHIR) without clinical neurodegenerative diseases were analyzed (Esterbauer et al., 2001). All human experiments were performed in accordance with the Helsinki declaration. Respective ethics committees approved study protocols (Prot. 0081260-BZ, Ethics Committee Bolzano, Italy; 415-EP/73/243–2013, Salzburg, Austria) and study subjects provided informed consent.

2.3. Animals

For measurements in the MPTP model, adult male and female C57BL/6 J mice (Janvier), weighing 25–30 g, kept under standard conditions and housed in groups of 4 in individually ventilated cage systems to protect the experimenter from MPTP exposure, received four doses of 12.5 mg/kg MPTP in 2 h intervals. Animals were sacrificed by neck dislocation before and at 30 min, 1, 2, 3 and 7 days after the completed MPTP injection protocol. Brain tissues, obtained from the frontal lobe, the cerebellum, the midbrain including the SN and the striatum, were quickly dissected on ice and snap-frozen in liquid nitrogen. Tissue samples of the same brain regions of 7–8 month old transgenic mice expressing the human α–synuclein harboring the A30P mutation under the control of the mouse Thy-1 promoter (B6; D2-Tg (Th-1-SNCA*A30P) lin44) were also collected. All animal procedures were approved by the respective government agency (Animal Experiment 09–016, Presidential Office of the Government Tübingen, Baden Würtenberg, Germany).

2.4. Dopamine measurements

Brain samples were homogenized by ultrasonification for 10 s in 1 ml 0.4 M perchloric acid and centrifuged at 22,000 ×*g* for 10 min at 4 °C. Supernatants were passed through a 0.2 μm filter (Minisart RC4, Sartorius). Dopamine levels were determined by high-performance liquid chromatography using an electrochemical detector and isocratic conditions (Buck and Ferger, 2008). The positions and areas of the peaks of the neurotransmitters of interest were compared with external standards using a standard calibration ranging from 10^{-9} to 10^{-6} M. The neurotransmitter amounts were expressed as ng/mg wet tissue weight.

2.5. RNA and protein extraction

Total RNA from post-mortem human and mouse brain tissues was extracted using QIAzol lysis reagent and the RNeasy Lipid Tissue Mini Kit (QIAGEN). Frozen tissues (30–100 mg) were placed into 2 ml tubes containing a 5 mm stainless steel bead, 700–1000 μl QIAzol was added and tissue was homogenized using a TissueLyzer (QIAGEN) twice at 20 Hz for 3 min. To obtain RNA and protein from the same sample, we used an optimized user-developed protocol (QIAGEN-RY16). After the addition of 140–200 μl chloroform homogenates were centrifuged at 12,000 x g for 20 min at 4 °C for phase separation. RNA was extracted from the upper aqueous layer using RNeasy spin columns according to the manufacturer's protocol. RNA concentration and integrity was measured using a Nanovue Spectrophotometer (GE Healthcare) and the QIAxcel Advanced Instrument (QIAGEN), respectively. RNA integrity scores of < 5 (two samples) were excluded. The remaining scores ranged between 5.0 and 6.8.

The phenol/ethanol supernatant containing the protein fraction was precipitated with 1.5 ml isopropanol, centrifuged at 12,000 x g for 10 min at 4 °C and the supernatant removed. The pellet was denatured with 2 ml guanidine-ethanol at room temperature for 20 min, centrifuged at 7500 x g for 5 min and the supernatant removed. The latter step was repeated twice. After incubating with 2 ml of 100% ethanol for 20 min, pellets were air-dried and dissolved in 10 M urea containing 50 mM dithiothreitol at room temperature for 1 h followed by alternate steps of incubation at 95 °C for 3 min and incubations on ice with periodic sonication (Sonoplus HB 27, Bandelin, Berlin), until proteins were completely dissolved. After centrifugation at 10,000 x g for 10 min at room temperature, protein concentrations of the supernatants were determined using the Bradford assay (Bio-Rad).

2.6. Real-Time qPCR

DNase I-treated total RNA (1 μg/reaction) was reverse transcribed with the QuantiTect Reverse Transcription (RT) kit (QIAGEN), using a mix of random hexamer and oligo-dT primers as described (Auer et al., 2012). cDNAs were amplified in duplicate by real-time PCR using Maxima SYBR Green (Thermo Scientific) or GoTaq™ qPCR Master Mix (Promega) and primers targeting exons B1 and B4 or B5 and exon 2, to quantify the two main CNS-specific *PPARGC1A* transcripts. RG transcripts were quantified using primers targeting exon 1 and exon 2. Primers targeting exon 5 and exon 7A or exon 2 and the extended part of exon 3 were used to measure the transcripts encoding the class of NT-PGC-1α isoforms or a short, putative dominant negative isoform, respectively (Supplementary Material, Fig. S1 for primer targets and Table S1 for primer sequences). To directly compare measurements of *PPARGC1A* transcripts by region, gene segments containing the sequences targeted by the respective transcript-specific assays were cloned and used for the construction of standard curves. The accuracy of the assays was verified by sequencing amplicons cloned from samples of three post-mortem cases. RNA levels of genes encoding glial fibrillary acidic protein (GFAP, Hs00909236_m1), tyrosine hydroxylase (TH, Hs00165941_m1), enolase 2 (ENO2, Hs00157360_m1), allograft inflammatory factor 1 (AIF1, Hs00610419_g1) and tumor necrosis factor alpha (Tnf, Mm 00443258_m1) were quantified using TaqMan gene expression assays (Applied Biosystems) listed in parentheses. RNA levels of the gene encoding microtubule associated protein 2 (MAP2) were amplified in duplicate by RT-PCR using Maxima SYBR Green or GoTaq™ qPCR Master Mix, the primers listed and the Rotor-Gene™Q (QIAGEN) instrument or the LightCycler™480 Instrument (Roche). Relative mRNA levels were calculated using the comparative threshold cycle method (ΔC_T). Constitutively expressed *RPLP0* (Ribosomal Protein, large, P0) RNA was used for normalization of mRNA abundance as described (Auer et al., 2012). To determine the validity of *RPLP0* as a reference gene, we also measured *CYC1* mRNA levels, previously shown to be stably expressed in brain regions from PD and controls (Rydbirk et al., 2016), in a subset of samples for comparison.

2.7. Plasmids

Plasmids used for *in vitro* transcription/translation included the coding sequences of the reference protein, B4-PGC-1α, B5-PGC-1α and the truncated isoforms NT-PGC-1α, B4-7a-PGC-1α, B5-7a-PGC-1α, E1-E3extended (ext), B4-E3ext and B5-E3ext cloned into the *Bam*HI/*Xho*I sites of the pT7CFE1-CHis vector (Thermo Scientific). Plasmids encoding the full length and NT transcripts were previously described (Soyal et al., 2012). Plasmids encoding B5-PGC-1α-GFP, B4-7a-PGC-1α-GFP or PGC-1α7a-GFP (also termed NT-PGC-1α-GFP) used for

immunocytochemistry have been described (Soyal et al., 2012). Primers for the 3ext transcripts are listed in Supplementary Material, Table S1. The human promoter-luciferase reporter vectors pCD36Prom-Luc and pPCK1-Prom-Luc and the expression plasmids pHNF4α and pPPARγ were previously described (Felder et al., 2011). The correct sequence was verified in all plasmids used.

2.8. In vitro transcription/translation

The 1-Step™ Human Coupled *in vitro* Transcription/Translation (IVT) Kit (Thermo Scientific) optimized for production of human proteins was used for synthesis of PGC-1α proteins. Circular pT7CFE1-CHis plasmids (approximately 1 μg) containing the sequences encoding PGC-1α isoforms were incubated with 12.5 μl HeLa cell lysates, 2.5 μl accessory proteins and 5 μl reaction mix for 4 h 30 min at 30 °C.

2.9. Immunoblotting and immunocytochemistry

In vitro transcription/translation products (4 μl reaction mixture) or proteins extracted from brain samples (40 μg) were denatured for 5 min at 95° C in sample buffer (75 mM Tris-HCl, pH 6.8, 4% *w/v* SDS, 10% glycerol, 50 mM dithiothreitol, 0.01% w/v bromophenol blue), cooled on ice and subjected to electrophoresis in 7–10% polyacrylamide gels. Separated proteins were transferred to polyvinylidene fluoride membranes (Bio-Rad) that were blocked with 1× Tris-buffered saline (TBS), pH 7.6, containing 10% Blotting grade Blocker (Bio-Rad) for 2 h at room temperature. Membranes were incubated with the primary antibodies, diluted 1: 400 in TBST (0.1% Tween 20 in 1xTBS) overnight at 4° C. Membranes were subsequently incubated for 1 h at room temperature with the respective secondary antibody (Goat anti-Rabbit or Goat anti-Mouse, IRDye 800 CW, LI-COR) and analyzed using the ODYSSEY infrared imager (LI-COR). Blots using only the secondary antibody served as negative controls. As loading controls, we used α-tubulin (Merck Millipore), β-actin (Cell Signaling) and/or coomassie staining of parallel gels. For densitometric analysis of Western blots the Image Studio™ software (LI-COR) was used.

Epitope-specific polyclonal antibodies were obtained to discriminate the various PGC-1α isoforms (Davids Biotechnology GmbH). Rabbits were immunized with MAWDMCNQDSESVWSDIE, MDETSPRLEEDWKKVLQREAGWQ and MDEGYF to obtain specific antibodies for the N-termini of the reference protein and the B5 or B4 isoforms, respectively. Antisera were affinity-purified using the respective peptides as ligands. Antibodies were tested using *in vitro* transcribed and translated products of clones encoding various isoforms and an in frame histidine-tag. The anti-exon 1 antibody correctly identified the translated full-length protein as well as NT-PGC-1α and E1E3ext, while isoforms initiated at B5 and B4 were not detected. The anti-B5 antibody identified all B5-initated isoforms, but failed to identify exon 1 and exon B4 initiated isoforms (Supplementary Material, Fig. S2). The anti-B4 antibody, directed against the very short B4-specific N-terminal sequence, failed to detect *in vitro* transcribed and translated isoforms. We used other peptides that contained the B4-specific epitope and extended into the coding region of exon 2 as antigens, but the antisera generated recognized a host of proteins. However, the initial anti-B4 antibody identified proteins of expected sizes in Western blots from human and mouse brain tissues. Moreover, the intensity of the selective bands was strongly reduced after pre-incubation with an excess of the immunization peptide (Supplementary Material, Figs. S3, S4, S5). Hence, it is likely that the B4-specific epitope is masked in the *in vitro* translated product that is initiated by a methionine residue located 8 residues upstream of the B4 amino-terminal methionine. In the latter protein, only two amino acids of the peptide MDEGYF were predicted to have a relative solvent accessibility above the 25% threshold (Scratch Protein Predictor. http://scratch.proteomics.ics.uci.edu/).

To further interrogate the specificity of the anti-B-4 and anti-B-5 antibodies, we used immunocytochemistry. SH-SY5Y and NT2/D1 cells obtained from ATCC were cultured in DMEM/F12 (Sigma-Aldrich) supplemented with 10% fetal bovine serum and 1% penicillin/streptomycin (Invitrogen). Cells were transfected with plasmid constructs encoding B5-PGC-1α-GFP, B4-7a-PGC-1α-GFP or PGC-1α7a-GFP (also termed Ex1-7a-GFP or NT-PGC-1α-GFP) for 24 h using DNAfectin™ (ABM Inc.). For microscopy, transfected cells were transferred to round glass slides (1.2 mm diameter), grown overnight, fixed with 4% paraformaldehyde for 30 min at room temperature, permeabilized with 0.2% Triton X-100 for 15 min, blocked in 3% bovine serum albumin (BSA) for 1 h and incubated with the primary antibody diluted with Hank's balanced solution (HBSS) and 0.1% BSA overnight at 4° C. On the next day, cells were washed 3× with HBSS and incubated with the secondary antibody (goat anti-rabbit IgG, Cy5 conjugated, Abcam), diluted 1:2500 with HBSS and 0.1% BSA for 1 h at room temperature. Nuclei were counterstained with 0.1 μg/ml 4`6-diaminidino-2-phenylindole (DAPI, Sigma-Aldrich) and slides were mounted in Mowiol/DAPCO (Sigma-Aldrich). Imaging of specimens was done by sequential acquisition with a Leica TCS SP5II AOBS confocal microscope (Leica Microsystems) equipped with a HCX PL APO 63×/1.4 oil immersion objective and controlled by the LAS AF SP5 software (Leica Microsystems). DAPI was excited with a diode laser (405 nm) and emission was detected between 430 and 480 nm. GFP was excited with the 488 nm line of the Argon laser and emission was detected in the 500–560 nm range. Cy5 was excited with the HeNe laser (633 nm) and emission was detected in the 645–780 nm range. Samples were imaged using 3 x zoom and a line average of 3. These experiments clearly showed that the anti-B4 antibody only detected cells transfected with pB4-PGC-1α7a and the anti-B5 antibody only detected cells transfected with B5-PGC-1α-GFP. Following pre-absorption of the antibody with the respective immunization peptide, the Cy5 signals were minimal or absent (Supplementary Material, Figs. S6 and S7).

2.10. Cell culture and transfection experiments

SH-SY5Y cells were plated in 24-well dishes one day before transfection and transfected with plasmid constructs for 24–48 h using DNAfectin™ (ABM Inc.). pRL-TK plasmid (Promega) was used as transfection control. Luciferase activities were measured using the Dual Luciferase Reporter Assay System (Promega) as described (Oberkofler et al., 2002). Results are means (SE) of three or more experiments, each performed in quadruplicate.

2.11. Genotyping

We typed rs17592631, rs11737023 and rs3966917, all localized in the brain-specific genomic *PPARGC1A* region, using TaqMan Genotyping Assays (Applied Biosystems). The respective typing reagents were C_32808047_10, C_473389_10 and C_26212324_10. The accuracy of typing was verified by sequencing of 10 alleles and repeat assays in 40 samples. In all cases, initial and repeat or sequence analyses showed identical results.

2.12. Statistical analysis

For comparison of categorical variables, we used a contingency χ^2-test. For comparison of specific transcript levels by brain region and/or disease, one- or two-way ANOVA was used. Logarithmic transformations were used if the equal variance and normality assumptions of ANOVA were rejected. Univariate associations were ascertained by linear correlation analysis or the *t*-test for independent samples. Measurements were adjusted for confounding effects as indicated. Allele frequencies were estimated by gene counting. Agreement with Hardy-Weinberg equilibrium was ascertained using a χ^2 goodness-of-fit test. Differences in genotype distributions between PD and controls were calculated using a χ^2 distribution. The THESIAS software (http://gencanvas.ecgene.net/downloads) was used to estimate standardized

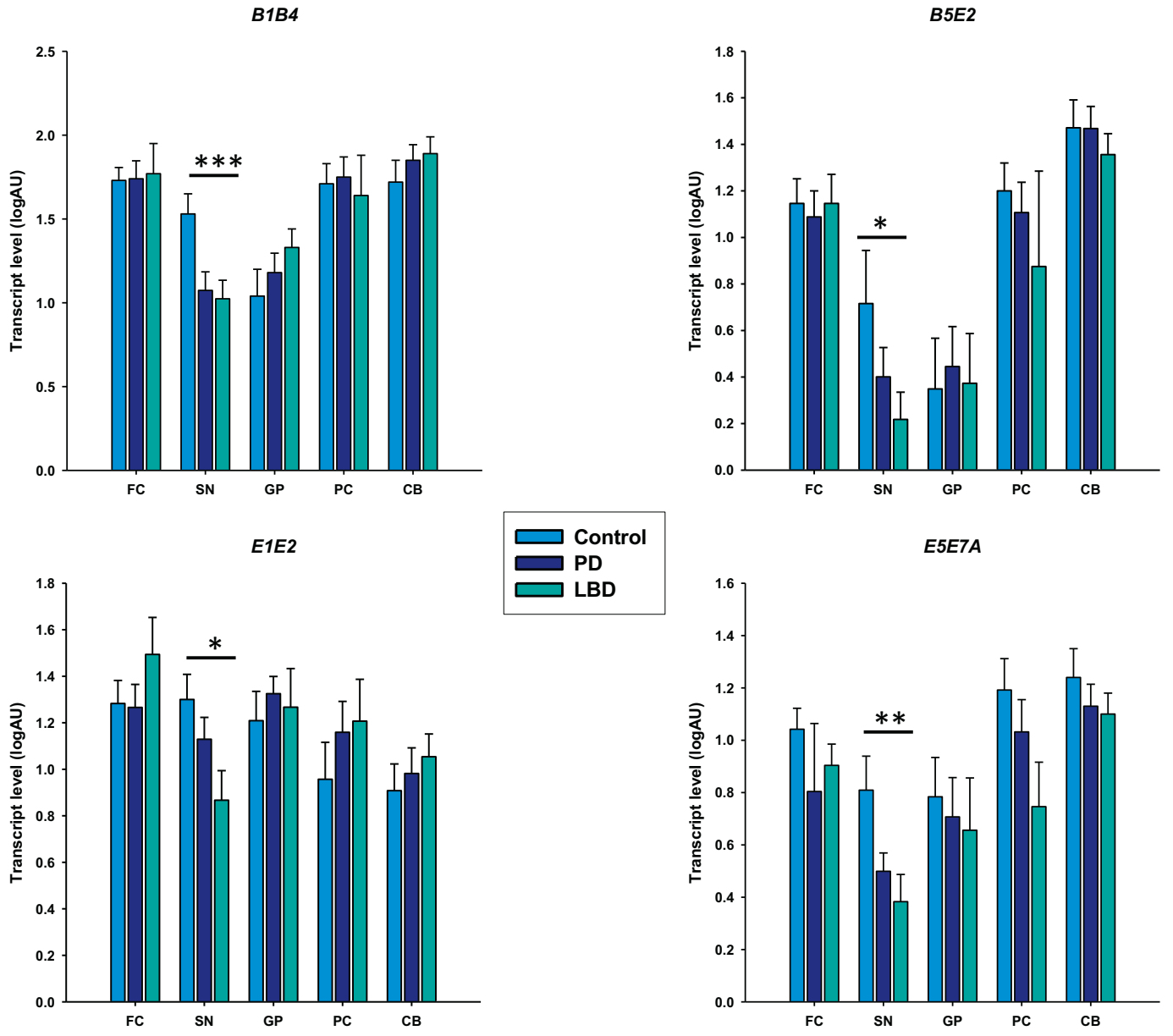

Fig. 1. Levels of *PPARGC1A* transcripts *B1B4*, *B5E2*, *E1E2* and *E5E7A* in post-mortem brain tissues from 13 controls, 21 Parkinson's disease and 8 Lewy body dementia cases. Columns (bars) are means (SE) of log-transformed transcript levels in arbitrary units (AU). Samples were collected from frontal cortex (FC), substantia nigra pars compacta (SN), globus pallidus (GP), parietal cortex (PC) and cerebellum (CB); *$P < .080$, **$P < .05$, ***$P < .01$.

pair-wise LD expressed in terms of D' and haplotype frequencies. Unadjusted and co-variate adjusted haplotype-phenotype parameters were estimated as OR for each haplotype being present with a predicted frequency > 1% by comparison to the most frequent haplotype. Two-sided *P*-values < .05 were considered statistically significant.

3. Results

3.1. Studies in post-mortem human tissues

CNS-specific *PPARGC1A* transcripts are initiated in exon B1 followed by exons B4 and/or B5 and exon 2–exon 13 (Soyal et al., 2012). Thus, measurements using primers targeting B1 and B4 include transcript structures *B1B4E2-E13* as well as *B1B4B5E2-E13*, while PCR reactions with primers targeting B5 and E2 include transcripts containing *B1B5E2-E13* and *B1B4B5E2-E13*. Primers targeting *E1E2* are specific for RG transcripts. Due to the primer selection in the upstream exons, splicing variants downstream of E2 are also included in the respective readouts. To directly quantify the variant encoding NT-PGC-1α, we used primers in E5 and E7A. Hence, the transcripts measured may have been initiated in B1 or E1 (Supplementary Material Fig. 1). RNA integrity scores showed no associations with age, sex, brain region, disease status or post-mortem time. Similarly, *RPLP0* levels used for normalization of transcript levels revealed no associations with age, sex or post-mortem time. However, two-way ANOVA using brain regions and control/PD/LPD status as independent variables showed a significant effect of region ($P < .005$), while no difference for disease status was noted ($P = .653$). Post-hoc analysis displayed lower ΔC_T values in the cerebellum than in the SNPC and the parietal cortex ($P < .05$), while ΔC_T values among the other brain regions did not differ (Supplementary Material, Fig. S8). Moreover, we compared differences in ΔC_T values of *RPLP0* and *CYC1* in 49 samples obtained from various brain regions of PD/LBD cases and controls and found no significant effect of PD/LBD/control status or brain regions (Supplementary Material, Fig. S9). Taken

together, these analyses suggest that the use of *RPLP0* as reference gene was justified. While a modest bias between transcripts in the cerebellum and SNPC or parietal cortex may have occurred, analyses of cerebellum tissue showed no associations with PD/LBD (see below). Irrespective of brain and *PPARGC1A* regions and case/control status, considerable variability in the levels of the *PPARGC1A* transcripts was observed. Univariate analyses of individual *PPARGC1A* transcripts showed no associations with age or sex, post-mortem time or RNA integrity. Two-way ANOVA with PD/LBD/control status and brain regions as independent and log-transformed mRNA levels adjusted for neurofibrillary tangle stages as dependent variables revealed no difference of global levels of the various *PPARGC1A* transcripts by disease status, but a strong effect of brain regions on transcript levels of *B1B4* and *B5E2* (both $P < .0001$). Both types of transcripts were less abundant in SNPC and globus pallidus than in the other brain regions. Compared with *B1B4* and *B5E2* transcripts, *E1E2* and *E5E7A* transcript levels differed by brain region to a lesser extent ($P = .0094$ and $P = .0008$), respectively. Post-hoc analysis revealed that *E1E2* transcript levels were lower in the SNPC and cerebellum than in the frontal cortex, while E5E7A transcript levels were higher in cerebellum than in SNPC and globus pallidus. Region specific analyses showed no significant differences of the various *PPARGC1A* transcripts by disease status in frontal and parietal cortex, globus pallidus and cerebellum. However, lower levels of *B1B4* ($P = .0055$) and *E5E7A* ($P = .0480$) and borderline lower levels of *B5E2* ($P < .0753$) and *E1E2* ($P = .0711$) of PD/LBD were observed in the SNPC (Fig. 1, Table 2). No associations of *PPARGC1A* transcripts in the SNPC were noted with age, sex, RNA integrity or post-mortem time.

We have previously shown in mouse brain cells (by semi-quantitative PCR) that the CNS-specific B4 containing transcripts are primarily expressed in neuronal cells and to a lesser extent in oligodendrocytes and microglia, but not, or only in minimal amounts in astrocytes. RG transcripts are expressed in astrocytes and neuronal cells and to a lesser extent in oligodendrocytes and microglia (Soyal et al., 2012). Hence, differences in transcript levels between controls and PD or LBD cases may result from changes in the cellular composition of tissue samples. Therefore, we measured mRNA levels of marker genes for astrocytes (*GFAP*), microglia (*AIF*), neurons (*ENO2, MAP2*) and dopaminergic neurons (*TH*) (Table 2). Levels of *GFAP* and *AIF* transcripts did not change with disease status in the SNPC, but transcript levels of *TH*, *MAP2* and *ENO2* were substantially reduced in PD and LBD cases. In going from controls to PD and/or LBD, transcript ratios of *B1B4* to *GFAP* decreased ($P < .05$), while ratios of *B1B4* to *AIF* and *ENO2* did not change significantly. However, transcript ratios of *B1B4* to *TH* or *MAP2* even increased ($P < .05$). These results are consistent with a predominant loss of dopaminergic neuronal cells in SNPC.

For studies on isoform expression, we used epitope-specific polyclonal antibodies, termed anti-E1, −B4 and −B5 and directed against the N termini of the reference PGC-1α and the CNS-specific isoforms with translation start codons in exon B4 and B5, respectively. In Western blots of protein extracts from the regions collected (Supplementary Material, Fig. S4), we noted differences in the intensities of bands by brain regions, but the antibody-specific protein patterns were similar among regions. We next analyzed the protein patterns in SNPC and globus pallidus from 14 PD and 9 control cases (Fig. 2). Again, we observed considerable variability in levels of protein isoforms in both PD and control. Generally, PGC-1α proteins were expressed at higher levels in SNPC than in globus pallidus. Although the sizes of the proteins detected by the three antibodies were in some cases similar considering small differences due to the N-terminal segments, their relative intensities showed marked differences. With the anti-E1 antibody, proteins migrating at 39 and 36 kDa (most likely NT-PGCs) showed the highest intensities, while those at 82 and 30 kDa or 55 and 17 kDa appeared to be most abundant with the anti-B5 or anti-B4 antibodies, respectively. The B5-epitope was present in several proteins. Proteins of similar sizes were also detected in SH-SY5Y or NTERA-2D1 cell extracts. Thus, generation of these bands by post-mortem degradation is unlikely. Given the large number of isoforms described or predicted by identified exon structures of *PPARGC1A* transcripts ((Martinez-Redondo et al., 2015) and (Supplementary Material, Table S2), not all bands that were strongly reduced in preincubation experiments with the respective immunization peptides could be clearly assigned to their transcript structure. For instance, the 55 kDa protein harboring the B4-epitope has recently been suggested to be non-specific (Ruas et al., 2012). However, this protein was selectively recognized by the anti-B4 antibody and may be encoded by RNA species with apparent sizes of 3.2 or 2.8 kb that we have detected in Northern blots of human brain RNA with probes consisting of CNS-specific exons B2-B5 and exons 2–7 (Soyal et al., Fig. 3A). Proteins with sizes expected for full-length reference, B4 and B5 proteins were also detected, but they were less abundant than the truncated isoforms. Proteolysis appeared to reduce the levels of some proteins, as post-mortem time was inversely associated with abundance levels of proteins detected with the anti-B5 antibody including the 100 kDa ($p = .001$), the 82 kDa ($P = .023$) and the 63 kDa ($p = .035$). Associations of post-mortem time with proteins detected with the anti-E1 and anti-B4 antibodies were not observed. Compared to controls, PD cases showed a greater abundance levels of B4–30 and B4–17 kDa proteins in the globus pallidus ($P < .05$). A similar trend for the B4–17 kDa protein was noted in SNPC ($P < .07$), while B4–30 kDa proteins were detected in the SNPC only in few cases. To substantiate these results, we measured *E2E3ext* transcripts likely to encode the 17 kDa isoform and observed higher levels in PD in comparison to controls in SNPC ($P = .008$) and globus pallidus ($P = .035$) (Fig. 3). No associations of *E2E3ext* transcript or 17 kDa isoprotein levels in SNPC or globus pallidus with age, sex, post-mortem time or RNA integrity were observed.

As the B4–17 kDa protein may represent an inhibitory isoform, we performed transient co-transfection studies in SHSY-5Y cells using the *PCK1* or the *CD36* promoter reporter plasmids along with expression vectors encoding HNF4α or PPARγ (Fig. 4). Plasmids encoding full-length PGC-1α isoforms with or without pB4-PGC-1α-3ext were co-transfected. PGC-1α was a stronger co-activator of HNF4α on the on the *PCK1* promoter in.

comparison to B5-PGC-1α, while no differences between the three full-length proteins were observed in PPARγ coactivation of the *CD36* promoter. The truncated B4-E3ext protein inhibited the co-activation of all three full-length proteins on both promoters in a dose dependent fashion.

Table 2
Transcript levels in substantia nigra pars compacta of post-mortem samples.

Transcripts	Control	PD	LBD	P^1	P^2	P^3
B1B4	1.47 (0.12)	0.96 (0.11)	0.97 (0.11)	0.0055	0.0368	0.0267
B5E2	0.70 (0.22)	0.38 (0.13)	0.10 (0.12)	0.0753	n.s.	0.0731
E1E2	1.31 (0.11)	1.07 (0.09)	0.89 (0.14)	0.0711	n.s.	0.0622
E5E7A	0.83 (0.139	0.51 (0.07)	0.40 (0.10)	0.0480	0.0935	0.0779
GFAP	3.43 (0.17)	3.21 (0.10)	2.99 (0.25)	0.1995	n.s.	n.s.
AIF1	1.59 (0.14)	1.47 (0.129	1.10 (0.19)	0.1322	n.s.	n.s.
TH	1.96 (0.23)	0.99 (0.18)	0.52 (0.26)	0.0010	0.0025	0.0011
MAP2	2.95 (0.18)	2.13 (0.13)	1.64 (0.15)	0.0001	0.0035	0.0002
ENO2	2.00 (0.14)	1.38 (0.12)	1.20 (0.17)	0.0005	0.0321	0.0013

Results are means (SE) of log-transformed transcript levels expressed in arbitrary units AU); P^1, Anova; P^2 and P^3, post-hoc comparisons of control *vs.* PD and *vs.* LBD, respectively.

3.2. Animal studies

Our previous studies described the presence of *B1b4* containing *Ppargc1a* transcripts in the CNS of mice (Soyal et al., 2012) and rats (unpublished). *B5e2* transcripts were not detected in mice and such transcripts would have a very short open reading frame of 11 amino acid residues. Tissue samples from brain regions of the MPTP mouse

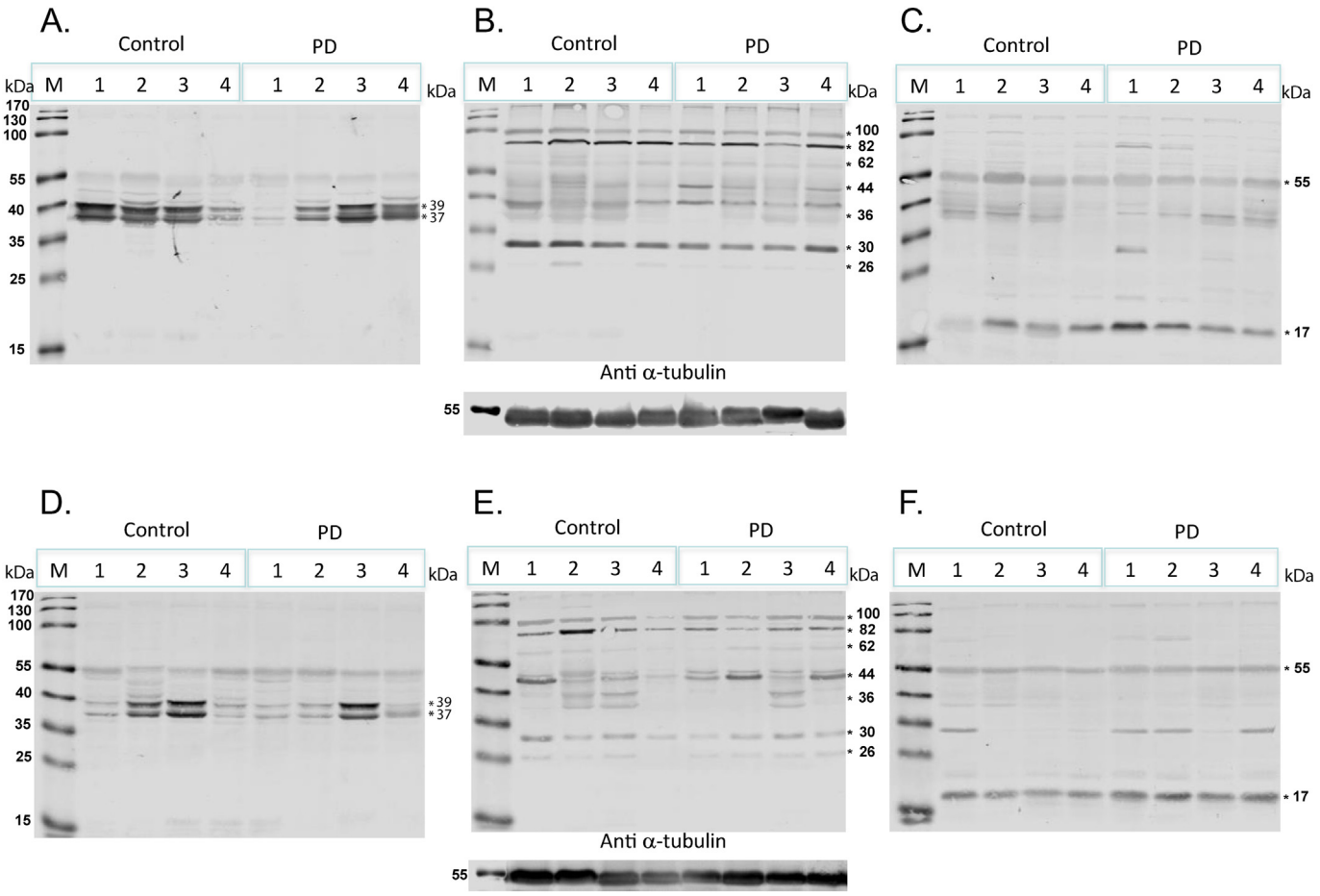

Fig. 2. PGC-1α isoforms encoded by reference gene and CNS-specific transcripts in post-mortem tissue of controls and Parkinson's disease cases. Western blots from SNPC (A, B, C) and globus pallidus (D, E, F) tissue extracts were probed with anti-E1 antibody specific for the N-terminal region of the reference protein (A, D), anti-B5 antibody, specific for one N-terminus of CNS-specific isoforms (B, E) or anti-B4, specific for the other N-terminus of CNS-specific isoforms (C, F). Western blots probed with anti-α-tubulin antibodies are shown below B and E. M shown on the left of blots refers to MW markers. Apparent MWs of bands that vanished or were greatly reduced in competition experiments with the respective immunization peptides are shown on the right of each blot. See also Supplementary Material, Fig. S6.

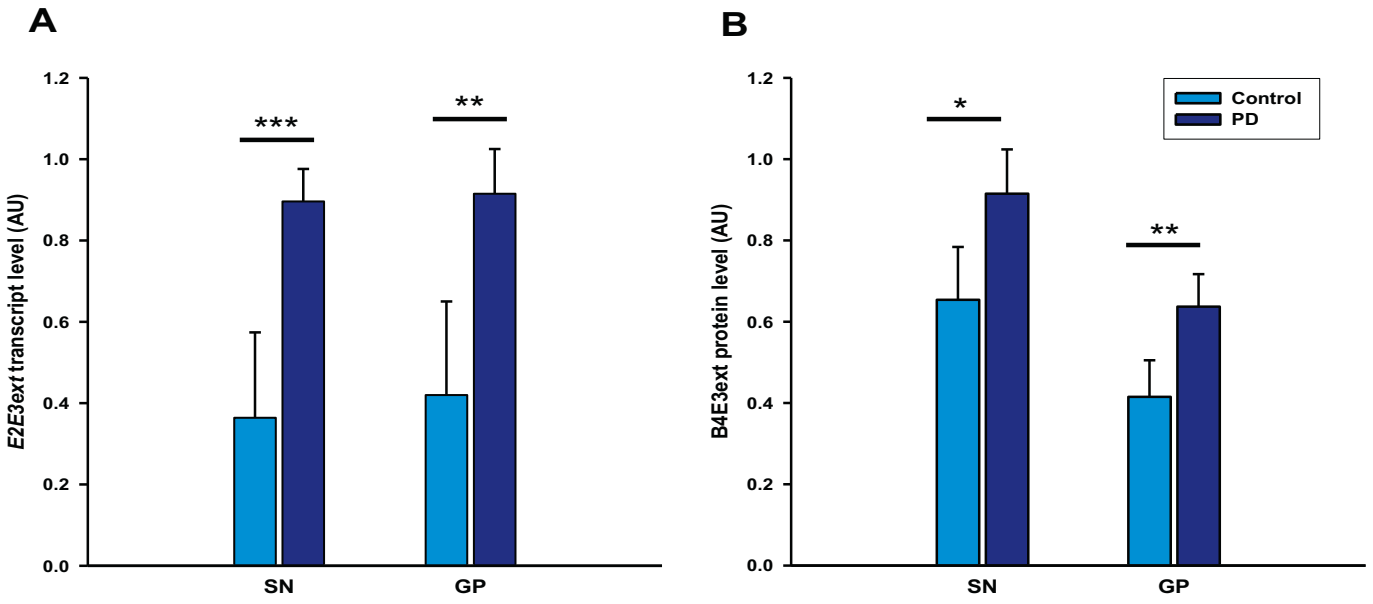

Fig. 3. Increased expression of 17 kDA proteins and their transcripts in PD. A) E2E3ext. transcript abundance levels in substantia nigra and globus pallidus of controls and PD cases; B) Expression levels of B4–17 kDa proteins in the respective regions. Results are means (SE). *P < .07, **P < .05, ***, P < .01.

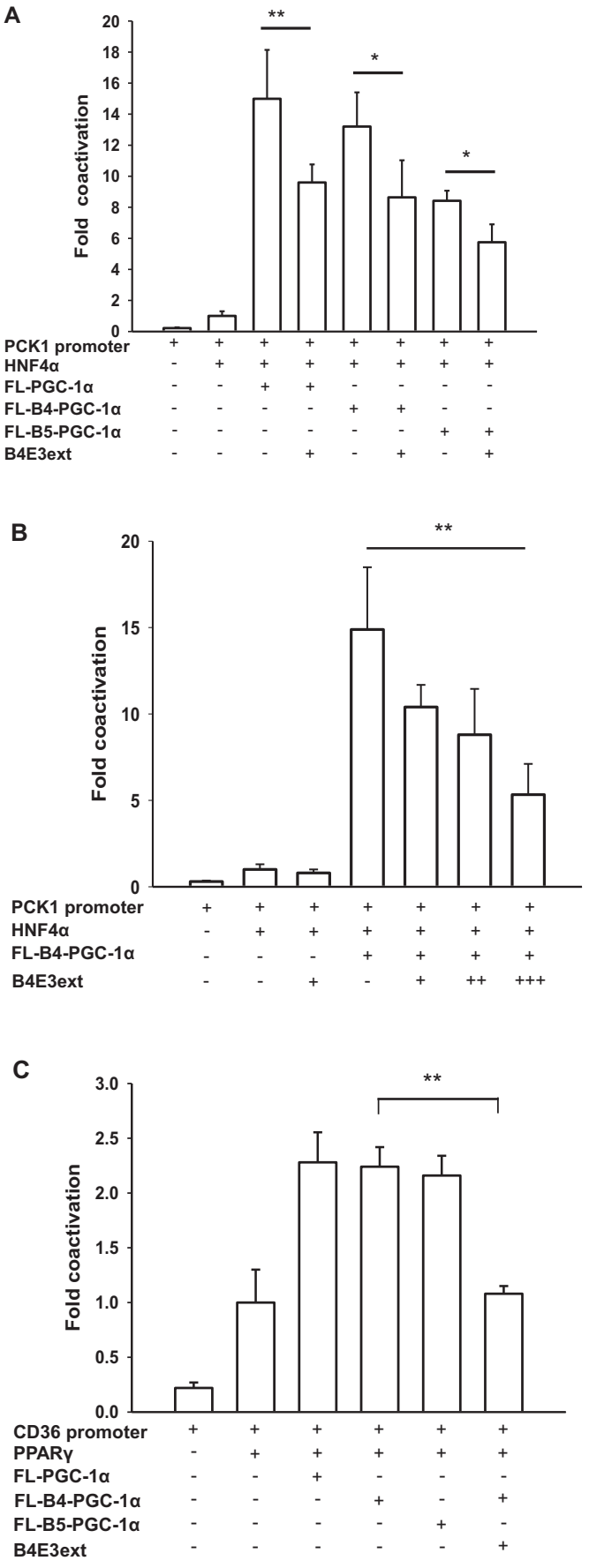

Fig. 4. The truncated 17 kDa CNS-specific isoform encoded by *B4E3ext* transcripts competitively inhibits the co-activation of HNF4α at the *PCK1* and PPARγ at the *CD36* promoters by full-length PGC-1α proteins. Activation of transfected *PCK1* promoter reporter plasmids by plasmids encoding HNF4α and full-length proteins PGC-1α, B4-PGC-1α or B5-PGC-1α without or with co-transfection of plasmids encoding B4-3Eext are compared (A). Co-transfection of plasmids encoding B4-E3ext does not activate HNF4α at the *PCK1* promoter and co-transfection of plasmids encoding full length B4- PGC-1α and equal, two- or threefold molar amounts of plasmids encoding B4-E3ext results in a dose-dependent inhibition of HNF4α co-activation by full-length proteins (B). The three full-length proteins show similar coactivation of PPARγ at the *CD36* promoter. Cotransfection of an equimolar amount of plasmids encoding B4-E3ext inhibits coactivation of FL-B4-PGC-1α (C). Fold coactivation is expressed relative to the transcriptional activities of HNFα or PPARγ at the respective promoters. Results are means (SE) of 3 to 5 experiments, each performed in quadruplicate. *P < .01, ** P < .005.

model were collected before and 30 min, 1, 2, 3 and 7 days after completion of the MPTP injection schedule. The MPTP treatment resulted in the expected dopamine decrease in the striatum and a surge in striatal *Tnfα* mRNA levels 24 h after the last dose (Fig. 5). Two-way analyses of transcript data revealed significant effects of time for both *B1b4* ($P < .0001$) and *E1e2* ($P = .0055$) transcripts, but the effect of region was only significant for *B1b4* ($P = .0001$). Analyses in individual brain regions showed significant decreases of *B1b4* and *E1e2* transcripts in all regions by time. Transcripts encoding the inhibitory 17 kDa isoform were detected only at very low levels. *Eno2* transcript levels measured in midbrain, frontal cortex and striatum also decreased by time ($P = .0003$) and *Th* transcript levels measured in midbrain decreased as well ($P = .0197$). Western blots showed altered expression of reference and CNS-PGC-1α isoforms (Supplementary Material, Fig. S5).

We next analyzed the transcript levels in genetically modified mice in which the human α-synuclein gene harboring the A30P mutation is expressed under the control of the mouse Thy-1 promoter (B6;D2-Tg (Thy1–1-SNCA*A30P)lin44). In comparison to wild-type mice, the transgenic mice displayed lower *B1b4* transcript levels in midbrain and striatum (both $P < .05$), while *E1e2* transcripts were markedly reduced in all four sampled regions, in particular, in the striatum (Fig. 6).

3.3. Genetic studies

To determine potential associations of the CNS-specific genomic region of *PPARGC1A*, we typed rs17592631, rs11737023 and rs3966917, all located far upstream of the RG promoter, in a cohort of PD and subjects without neurodegenerative disorders from the South Tyrolean region. To increase power, we typed participants from the SAPHIR study free of neurodegenerative diseases (Supplementary Material, Table S2). The augmentation of the control group was justified, as haplotype frequencies did not differ between controls from South Tyrol and Salzburg (Supplementary Material, Table S3). All polymorphisms fulfilled Hardy-Weinberg expectations. In the combined sample, frequencies of the more common alleles associated with rs17592631, rs11737023 and rs3966917 were 0.903, 0.771 and 0.807, respectively. These frequencies compare well with the respective frequencies in the European HAPMAP sample (0.905, 0.7806 and 0.814). Genotype distributions associated with any of the three SNPs did not differ between control and PD cases in the clinical, the post-mortem or the combined sample (Supplementary Material, Table S4). Haplotype analysis revealed 7 haplotypes that occurred with a frequency > 0.01. The test for global associations between haplotypes and PD was significant in the clinical sample ($\chi^2 = 14.204$, 6 df, $P = .0275$) and in the combined samples ($\chi^2 = 19.642$, 6 df, $P = .0030$), but not in the smaller post-mortem sample ($\chi^2 = 9.244$, 6 df, $P = .1614$). In particular, haplotype 111 was more and haplotype 112 was less frequent in cases than in controls. Haplotype 112 was associated with lower risk of disease in both the clinical and the post-mortem samples. In the

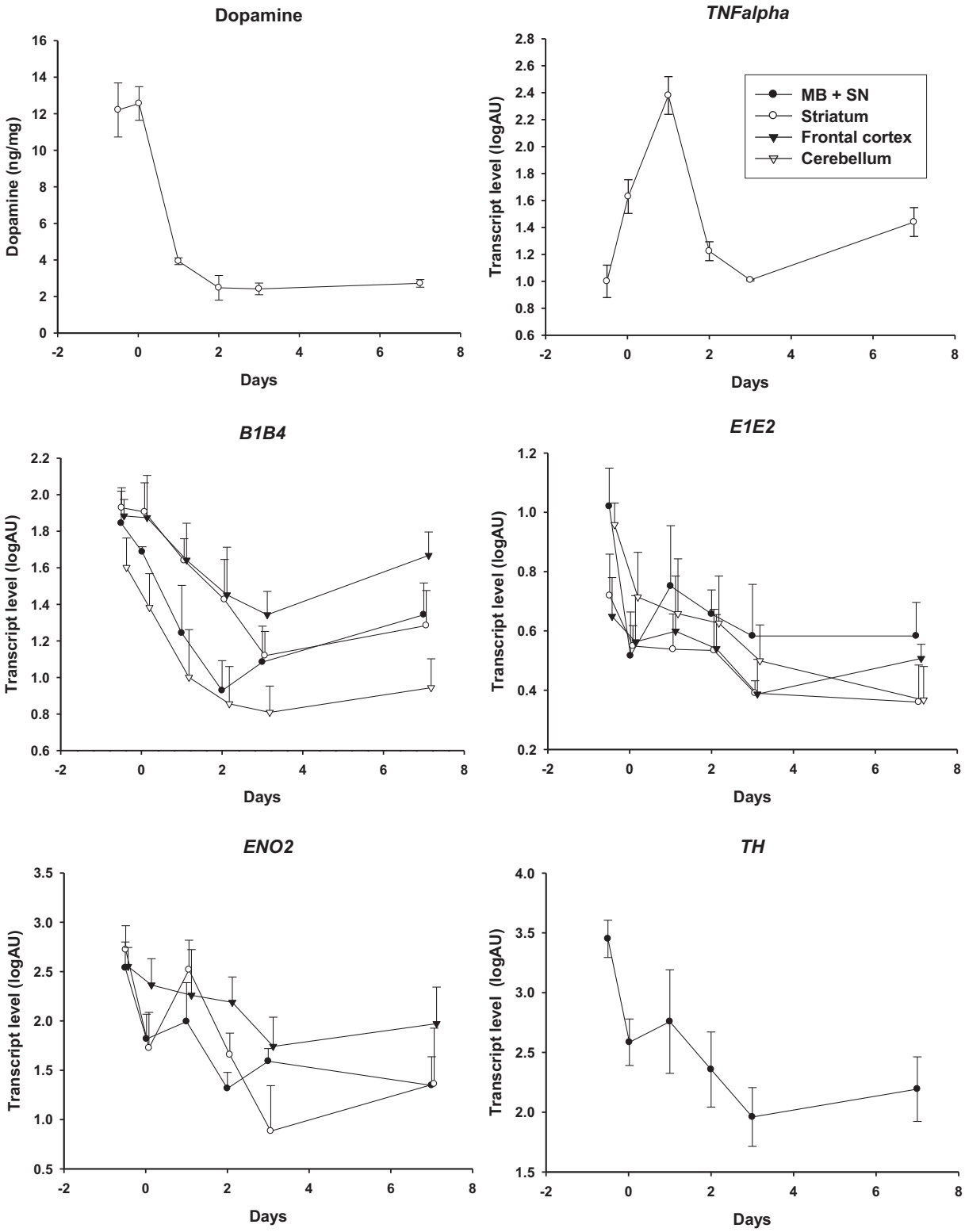

Fig. 5. Effect of MPTP administration on dopamine and various transcript levels in several brain regions. Samples from brain regions were obtained before and 30 min, 1, 2, 3 and 7 days after completion of the MPTP injection schedule. Decreases of tissue levels with time were significant for dopamine and *B1b4*, *E1e2*, *Eno2* and *Th* transcripts with the exception of *B1b4* transcripts in the frontal cortex at the 7 day time point. Results are means (SE) of dopamine or log-transformed transcript levels from 3 to 6 animals per time point. MB + SN = midbrain plus substantia nigra.

combined sample, haplotype 121 was also associated with lower disease risk (Table 3). For the three most common haplotypes (111, 112 and 121) that drive the association signal with PD the squared correlation between true and predicted haplotype dose was > 0.88.

To ascertain the specificity of the haplotype distribution for PD, we also determined the haplotype distribution of post-mortem AD disease cases. Unlike in PD, haplotype distributions defined by the same SNPs were very similar in AD cases and controls (Supplementary Material,

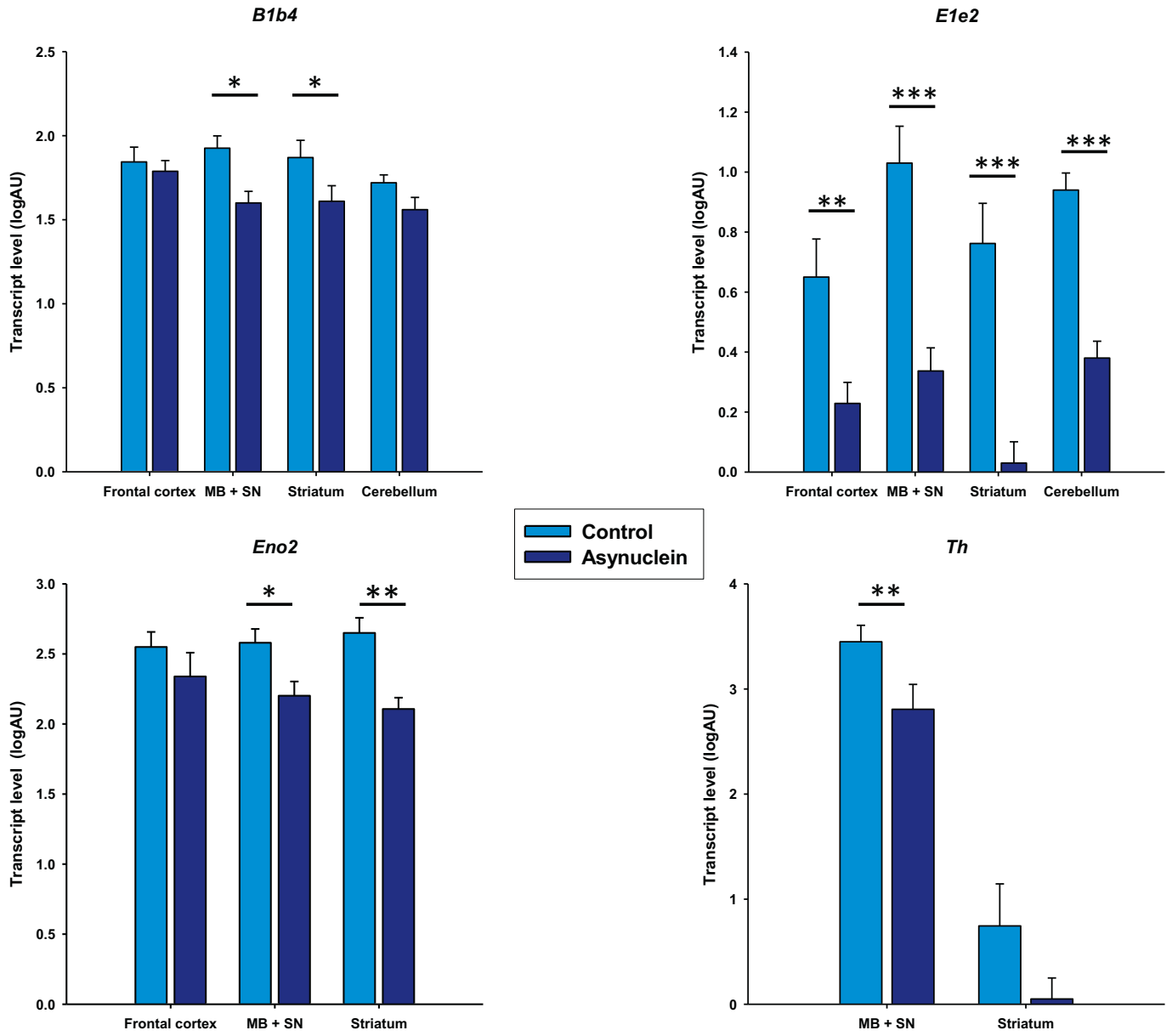

Fig. 6. Overexpression of the human α-synuclein A30P mutation in mice is associated with a strong reduction of *E1e2* transcripts. Tissue samples were obtained from the frontal cortex, midbrain including substantia nigra, striatum and cerebellum. Results are means (SE) of log-transformed transcript levels of 4–5 mice per group. *P < .05; **P < .01; ***P < .001; MB + SN = midbrain plus substantia nigra.

Table S5).

4. Discussion

Studies in mice have shown that adult conditional knockout of exon 3–5 of *Ppargc1a*, which targets reference as well as all B4-containing CNS-specific isoforms, leads to loss of dopaminergic neurons in the SNPC and robust amphetamine-induced ipsilateral rotation (Jiang et al., 2016). Similar results have been demonstrated in rats (Zheng et al., 2017). Upper vertebrates have an expanded repertoire of CNS-transcripts (including B5 containing transcripts) that are not expressed in mice or rats and may allow for a more finely tuned neuronal survival program in response to stress. Our human post-mortem studies extend previous studies by including the main encoding transcripts and show marked differences in the distribution of the CNS-specific transcripts *B1B4* and *B5E2* among the brain regions analyzed, while the distribution of RG transcripts is much less influenced by region. Intriguingly, the lowest levels of CNS-transcripts were noted in globus pallidus and SNPC thought to be very sensitive to toxic insults and/or energetic defects (Obeso et al., 2017). Significant or borderline reductions in the SNPC were noted for *B1B4* and *E5E7A* or *B5E2* and *E1E2* transcripts, respectively, while changes of any of the transcripts in other brain regions were not significant. Reduced levels of *PPARGC1A* transcripts in SNPC were reported recently in PD without details about the targeted gene regions (Su et al., 2015). Another study reported reduced levels of *E1E2* and B1B4 transcripts in PD (Eschbach et al., 2015). Similar to the latter study, the variability of transcript levels was large and may not only result from inter-individual variability, disease heterogeneity and tissue sampling, but pre-terminal insults such as hypoxia, as we have experimental evidence for differences in the regulation of transcription from the CNS and RG promoters by various signaling pathways including hypoxia (Soyal SM and Patsch W, unpublished). As our study was performed in SNPC tissue and neuronal markers were substantially decreased, the reduction of CNS-specific transcripts in PD and LBD may

Table 3
CNS-specific *PPARGC1A* haplotypes and Parkinson's disease.

Haplotype*	Clinical sample				Post-mortem sample				All			
	Control (790)	PD (196)	OR (95% CI)	P	Control (169)	PD (85)	OR (95% CI)	P	Control (959)	PD (281)	OR (95% CI)	P
111	0.611	0.681	reference		0.585	0.667	reference		0.607	0.677	reference	
112	0.138	0.078	0.51 (0.33–0.77)	0.0013	0.176	0.112	0.54 (0.30–0.97)	0.0383	0.144	0.088	0.53 (0.38–0.74)	0.0002
121	0.133	0.095	0.64 (0.44–0.93)	0.0201	0.123	0.085	0.57 (0.26–1.24)	0.1544	0.131	0.094	0.64 (0.46–0.90)	0.0108
122	0.026	0.043	1.45 (0.70–2.98)	0.310	0.007	0.018	3.57 (0.37–33.63)	0.2657	0.024	0.034	1.39 (0.70–2.76)	0.3405
211	0.008	0.018	1.83 (0.06–5.55)	0.2842	0.017	0.027	1.34 (0.35–5.14)	0.6656	0.010	0.020	1.66 (0.69–3.99)	0.2570
221	0.046	0.041	0.75 (0.42–1.37)	0.3549	0.077	0.045	0.47 (0.18–1.23)	0.1240	0.052	0.040	0.63 (0.38–1.05)	0.0756
222	0.033	0.035	0.95 (0.48–1.48)	0.8907	0.0150	0.046	1.97 (0.69–5.63)	0.2063	0.029	0.040	1.18 (0.68–2.05)	0.5504

Haplotype frequencies in controls and PD cases; ORs are relative to the most common haplotype; $P = .00301$ for global haplotype. Effects in the combined sample. *1 or 2 refers to the major or minor alleles, respectively, in the following order: rs17592631 C/T; rs11737023 G/A and rs3966917A/G.

result simply from a loss of dopaminergic neurons that express them and modest changes in promoter regulation. Nevertheless, the data in mice show that these transcripts may be themselves required for dopaminergic neuronal survival. As Lewy bodies were required for the PD diagnosis in our study, forms of PD that are not necessarily associated with Lewy bodies (Doherty et al., 2013; Kalia and Kalia, 2015) may have different *PPARGC1A* expression profiles. For instance, in Parkin-associated PD, PARIS, a substrate for the E3 ubiquitin ligase Parkin, accumulates, represses transcription from the PGC-1α promoter and causes selective loss of dopaminergic neurons in the SN that can be abrogated by overexpression of PGC-1α (Shin et al., 2011).

The reductions in specific *PPARGC1A* transcripts and transcripts of cell-specific markers tended to be more pronounced in LBD in comparison to PD, but only *MAP2* and *ENO2* transcripts were significantly lower in LBD. These results are in keeping with strong overlaps in the clinical picture and neuropathology of LBD and PD and the view, that these disorders may reflect specific entities of a continuous disease spectrum termed alpha-synucleinopathies (Lippa et al., 2007).

The analyses of proteins revealed multiple bands with differences between the antibodies used. Not all bands could be clearly assigned to the transcript structures that have been identified so far. Post-mortem degradation of proteins may have contributed to low levels of some proteins. It is also possible that other proteins contained epitopes used for generation of antisera. Hence, we can not exclude that some proteins identified by competition assays are not PGC-1a isoforms. However, using the eukaryotic gene prediction tool Gnomon (http://wwwncbinlmnihgov/RefSeq/Gnomon-descriptionpdf), additional new B5-initiated isoforms have been predicted from the human genomic sequence that are supported by mRNA and EST evidence in the NCBI database (entries XP_011512071, XP_005248191) and have predicted MW of 77.2 and 79.8 kDa. Furthermore, multiple bands have been detected in neuronal cell lines with other antibodies directed against the N-terminal region of PGC-1α (Hasegawa et al., 2016; Ye et al., 2017; Ye et al., 2016).

An exciting and potentially important result was the PD-associated increase of the 17 kDa bands detected with the anti-B4 antibody and likely representing the translation product of *B4-E3ext* transcripts. A similar protein initiated at an alternative transcription site has been reported in another study (http://scholarscompass.vcu.edu/etd/3225/). The respective protein lacks the second LXXLL motif that serves as an interaction site for several nuclear receptors including HNF4α. The truncated proteins also lack nuclear localization signals, but their size < 20 kDa should not impede their diffusion through the nuclear pore complex (Cyert, 2001). Indeed, we show now that the B4-PGC1-α3ext inhibits the co-activation of several promoters by full-length CNS-specific and reference proteins. As co-activation of PPARγ whose interaction site has been mapped distal to the second LXXL motif was also inhibited, heterodimerization and/or competition of truncated and full-length proteins for factors that enhance the co-activation properties of PGC-1α such as SRC-1 and p300 are likely modes of inhibition (Puigserver et al., 1999). A genome-wide expression study conducted in part in laser-captured dopaminergic neurons found that a set of 425 PGC-1α-responsive genes was significantly under-expressed in PD (Zheng et al., 2010). Two other studies using laser microdissection reported no significant reduction of *PPARGC1A* transcripts or PGC-1α immunoreactivity in substantia nigra neurons (Dolle et al., 2016; Simunovic et al., 2009). Thus, in sum these studies would suggest that the transcriptional function of PGC-1α is compromised in idiopathic PD despite moderated, if any reductions in its expression. It is therefore conceivable that the 17 kDa protein may contribute to the functional impairment observed in PD. However, additional studies are required to support the hypothesis that such a mechanism contributes to the pathogenesis of PD.

Full-length CNS- and RG-PGC-1α displayed subtle differences in co-activation of HNF4α at the *PCK1*, but not of PPARγ at the *CD36* promoter. Previous studies showed that alternative PGC-1α isoforms display distinct transcriptional regulation and protein stability. The N-terminal activation and repression domains, but not the RS/RNA recognition motifs appeared to determine gene programs as well as splicing events that are specifically regulated by some isoforms (Martinez-Redondo et al., 2016). Furthermore, an interaction of Necdin with the N-terminal region resulted in increased stabilization of PGC-1α and enhanced mitochondrial function in primary neurons (Hasegawa et al., 2016). Whether the CNS-specific isoforms that possess distinct N-termini differ from the reference proteins in their transcriptional co-activation and splicing program, is currently under study.

The MPTP metabolite 1-methyl-4-phenylpyridinium induced Parkinsonism in young drug addicts (Langston et al., 1983) and has been identified as a complex 1 inhibitor (Cleeter et al., 1992). Animal models based on MPTP intoxication have been used as valuable tools to study deficiencies in dopaminergic neurons, even though such models do not fully recapitulate human PD. Our studies in the acute MPTP model showed that dopamine levels decreased more rapidly and to a greater extent than *TH* mRNA levels. This finding is consistent with studies showing that the decrement in dopamine levels exceeds the loss of dopaminergic neurons in PD and that nitration of striatal TH that results in loss of enzymatic activity is induced by MPTP administration (Ara et al., 1998). Like in human brain tissues, transcript levels of *B1b4*

in mice were more abundant than levels of *E1e2* (Soyal et al., 2012; Szalardy et al., 2016). Unlike in human post-mortem tissues, the decrease of *B1b4* and *E1e2* transcripts along with a decrease in *Eno2* occurred in all brain regions studied suggesting a more general toxicity of the MPTP treatment in our animal model. Transgenic mice overexpressing the α-synuclein A30P mutation revealed moderately reduced mRNA levels of *B1b4* and *Eno2* transcripts in midbrain and striatum. However, reductions of *E1e2* transcript levels were substantial in all brain regions, particularly in the striatum, and may result from down-regulation of the RG promoter activity by α-synuclein (Siddiqui et al., 2012).

Our genetic studies showing consistent results in two populations suggest that the genomic region encompassing the CNS promoter and CNS-specific exons contributes to the pathogenesis of PD. Like in previous genome-wide association studies (GWAS), no associations of PD with individual SNPs were observed, but haplotypes typically are not reported in GWAS. The mechanisms whereby some haplotypes exhibit protective effects are not known, but may include the expression levels of specific isoforms in response to distinct signaling mechanisms. Importantly, some GWAS showed associations of the CNS-specific genomic region of *PPARGC1A* with phenotypes that are often encountered in PD. In subjects of European ancestry, a strong association of rs17590046, located between exons B1 and B4, with essential tremor (P-value $< 10^{-9}$) was reported (Muller et al., 2016) and confirmed in an Asian population (Xiao et al., 2017). Furthermore, a borderline significant association of rs16875528, also positioned between B1 and B4, with the sense of smell among US older adults (P-value = 9.10^{-6}) was observed (Dong et al., 2015). Our results must be cautiously interpreted, as a predicted, but not characterized locus lies in the same genomic region (LOC729175, NCB reference sequence XPP_001129558.1). Between amino acids 80–253, the predicted protein contains a domain exhibiting homology to DNA polymerase gamma and tau. The hypothetical mRNA is transcribed from the same strand and in the same direction as the CNS-*PPARGC1A* transcripts. EST clones have been observed in ES cells (Genbank Nr. CN283176) that overlap exon B1. We also observed similar transcripts in induced pluripotent stem cells and, to a lesser extent, in human brain tissue. Further characterization of LOC729175 is required, as variants of genes involved in mtDNA maintenance such as mtDNA polymerase gamma increase the risk of PD (Luoma et al., 2007).

5. Conclusion

Taken together, a link between the CNS-specific *PPARGC1A* locus and idiopathic PD is supported by higher expression levels of 17 kDa proteins and their encoding transcripts in SNPC and globus pallidus of PD in comparison to controls. The 17 kDa proteins inhibit the coactivation function of full-length PGC-1α and may therefore contribute to functional impairment of full-length PGC-1α in PD reported by others. In additon, genetic studies revealed protective haplotypes at the CNS-specific region of the *PPARGC1A* locus further supporting a role in PD.

Competing interest

The authors declare no competing financial interests.

Funding sources

This study was supported from the Fonds zur Förderung der wissenschaftlichen Forschung (FWF Project V344-B24, Elise Richter Programme) to S.S., MJFOX foundation (RRIA 2012) to W.P., the Paracelsus Medical University Salzburg (Projects E-13/18/094_PAT) to W.P. and (PMU-FFA-14/01/011-SOY) to S.S.

Appendix A. Supplementary data

Supplementary data to this article can be found online at https://doi.org/10.1016/j.nbd.2018.09.016.

References

Abeliovich, A., Gitler, A.D., 2016. Defects in trafficking bridge Parkinson's disease pathology and genetics. Nature 539, 207–216.
Ara, J., et al., 1998. Inactivation of tyrosine hydroxylase by nitration following exposure to peroxynitrite and 1-methyl-4-phenyl-1,2,3,6-tetrahydropyridine (MPTP). Proc Natl Acad Sci U S A 95, 7659–7663.
Auer, S., et al., 2012. Potential role of upstream stimulatory factor 1 gene variant in familial combined hyperlipidemia and related disorders. Arterioscler Thromb Vasc Biol 32, 1535–1544.
Braak, H., Braak, E., 1991. Neuropathological stageing of Alzheimer-related changes. Acta Neuropathol 82, 239–259.
Braak, H., et al., 2003. Staging of brain pathology related to sporadic Parkinson's disease. Neurobiol Aging 24, 197–211.
Buck, K., Ferger, B., 2008. Intrastriatal inhibition of aromatic amino acid decarboxylase prevents l-DOPA-induced dyskinesia: a bilateral reverse in vivo microdialysis study in 6-hydroxydopamine lesioned rats. Neurobiol Dis 29, 210–220.
Cleeter, M.W., Cooper, J.M., Schapira, A.H., 1992. Irreversible inhibition of mitochondrial complex I by 1-methyl-4-phenylpyridinium: evidence for free radical involvement. J Neurochem 58, 786–789.
Cyert, M.S., 2001. Regulation of nuclear localization during signaling. J Biol Chem 276, 20805–20808.
Doherty, K.M., et al., 2013. Parkin disease: a clinicopathologic entity? JAMA Neurol 70, 571–579.
Dolle, C., et al., 2016. Defective mitochondrial DNA homeostasis in the substantia nigra in Parkinson disease. Nat Commun 7, 13548.
Dong, J., et al., 2015. Genome-wide Meta-analysis on the Sense of Smell Among US Older Adults. Medicine (Baltimore) 94, e1892.
Dorsey, E.R., et al., 2007. Projected number of people with Parkinson disease in the most populous nations, 2005 through 2030. Neurology 68, 384–386.
Ebrahim, A.S., Ko, L.W., Yen, S.H., 2010. Reduced expression of peroxisome-proliferator activated receptor gamma coactivator-1alpha enhances alpha-synuclein oligomerization and down regulates AKT/GSK3beta signaling pathway in human neuronal cells that inducibly express alpha-synuclein. Neurosci Lett 473, 120–125.
Ekstrand, M.I., et al., 2007. Progressive parkinsonism in mice with respiratory-chain-deficient dopamine neurons. Proc Natl Acad Sci U S A 104, 1325–1330.
Eschbach, J., et al., 2013. PGC-1alpha is a male-specific disease modifier of human and experimental amyotrophic lateral sclerosis. Hum Mol Genet 22, 3477–3484.
Eschbach, J., et al., 2015. Mutual exacerbation of peroxisome proliferator-activated receptor gamma coactivator 1alpha deregulation and alpha-synuclein oligomerization. Ann Neurol 77, 15–32.
Esterbauer, H., Oberkofler, H., Krempler, F., Patsch, W., 1999. Human peroxisome proliferator activated receptor gamma coactivator 1 (PPARGC1) gene: cDNA sequence, genomic organization, chromosomal localization, and tissue expression. Genomics 62, 98–102.
Esterbauer, H., et al., 2001. A common polymorphism in the promoter of UCP2 is associated with decreased risk of obesity in middle-aged humans. Nat Genet 28, 178–183.
Felder, T.K., et al., 2011. Characterization of novel peroxisome proliferator-activated receptor gamma coactivator-1alpha (PGC-1alpha) isoform in human liver. J Biol Chem 286, 42923–42936.
Handschin, C., Spiegelman, B.M., 2006. Peroxisome proliferator-activated receptor gamma coactivator 1 coactivators, energy homeostasis, and metabolism. Endocr Rev 27, 728–735.
Hasegawa, K., et al., 2016. Promotion of mitochondrial biogenesis by necdin protects neurons against mitochondrial insults. Nat Commun 7, 10943.
Hely, M.A., Reid, W.G., Adena, M.A., Halliday, G.M., Morris, J.G., 2008. The Sydney multicenter study of Parkinson's disease: the inevitability of dementia at 20 years. Mov Disord 23, 837–844.
International Parkinson Disease Genomics, C., Nalls, et al., 2011. Imputation of sequence variants for identification of genetic risks for Parkinson's disease: a meta-analysis of genome-wide association studies. Lancet 377, 641–649.
Jiang, H., et al., 2016. Adult Conditional Knockout of PGC-1alpha Leads to Loss of Dopamine Neurons. eNeuro 3.
Kalia, L.V., Kalia, S.K., 2015. alpha-Synuclein and Lewy pathology in Parkinson's disease. Curr Opin Neurol 28, 375–381.
Kalia, L.V., Lang, A.E., 2015. Parkinson's disease. Lancet 386, 896–912.
Langston, J.W., Ballard, P., Tetrud, J.W., Irwin, I., 1983. Chronic Parkinsonism in humans due to a product of meperidine-analog synthesis. Science 219, 979–980.
Lin, M.T., Beal, M.F., 2006. Mitochondrial dysfunction and oxidative stress in neurodegenerative diseases. Nature 443, 787–795.
Lin, J., Handschin, C., Spiegelman, B.M., 2005. Metabolic control through the PGC-1 family of transcription coactivators. Cell Metab 1, 361–370.
Lippa, C.F., et al., 2007. DLB and PDD boundary issues: diagnosis, treatment, molecular pathology, and biomarkers. Neurology 68, 812–819.
Luoma, P.T., et al., 2007. Mitochondrial DNA polymerase gamma variants in idiopathic sporadic Parkinson disease. Neurology 69, 1152–1159.
Martinez-Redondo, V., Pettersson, A.T., Ruas, J.L., 2015. The hitchhiker's guide to PGC-1alpha isoform structure and biological functions. Diabetologia 58, 1969–1977.
Martinez-Redondo, et al., 2016. Peroxisome Proliferator-activated Receptor gamma

Coactivator-1 alpha Isoforms Selectively Regulate Multiple Splicing Events on Target Genes. J Biol Chem 291, 15169–15184.
McKeith, I.G., et al., 2005. Diagnosis and management of dementia with Lewy bodies: third report of the DLB Consortium. Neurology 65, 1863–1872.
Mudo, G., et al., 2012. Transgenic expression and activation of PGC-1alpha protect dopaminergic neurons in the MPTP mouse model of Parkinson's disease. Cell Mol Life Sci 69, 1153–1165.
Muller, S.H., et al., 2016. Genome-wide association study in essential tremor identifies three new loci. Brain 139, 3163–3169.
Nalls, M.A., et al., 2014. Large-scale meta-analysis of genome-wide association data identifies six new risk loci for Parkinson's disease. Nat Genet 46, 989–993.
Oberkofler, H., et al., 2002. Peroxisome proliferator-activated receptor (PPAR) gamma coactivator-1 recruitment regulates PPAR subtype specificity. J Biol Chem 277, 16750–16757.
Obeso, J.A., et al., 2017. Past, present, and future of Parkinson's disease: A special essay on the 200th Anniversary of the Shaking Palsy. Mov Disord 32, 1264–1310.
Puigserver, P., et al., 1999. Activation of PPARgamma coactivator-1 through transcription factor docking. Science 286, 1368–1371.
Ruas, J.L., et al., 2012. A PGC-1alpha isoform induced by resistance training regulates skeletal muscle hypertrophy. Cell 151, 1319–1331.
Rydbirk, R., et al., 2016. Assessment of brain reference genes for RT-qPCR studies in neurodegenerative diseases. Sci Rep 6, 37116.
Shin, J.H., et al., 2011. PARIS (ZNF746) repression of PGC-1alpha contributes to neurodegeneration in Parkinson's disease. Cell 144, 689–702.
Siddiqui, A., et al., 2012. Selective binding of nuclear alpha-synuclein to the PGC1alpha promoter under conditions of oxidative stress may contribute to losses in mitochondrial function: implications for Parkinson's disease. Free Radic Biol Med 53, 993–1003.
Simunovic, F., et al., 2009. Gene expression profiling of substantia nigra dopamine neurons: further insights into Parkinson's disease pathology. Brain 132, 1795–1809.
Soyal, S., Krempler, F., Oberkofler, H., Patsch, W., 2006. PGC-1alpha: a potent transcriptional cofactor involved in the pathogenesis of type 2 diabetes. Diabetologia 49, 1477–1488.
Soyal, S.M., et al., 2012. A greatly extended PPARGC1A genomic locus encodes several new brain-specific isoforms and influences Huntington disease age of onset. Hum Mol Genet 21, 3461–3473.
Spillantini, M.G., et al., 1997. Alpha-synuclein in Lewy bodies. Nature 388, 839–840.
St-Pierre, J., et al., 2006. Suppression of reactive oxygen species and neurodegeneration by the PGC-1 transcriptional coactivators. Cell 127, 397–408.
Su, X., et al., 2015. PGC-1alpha Promoter Methylation in Parkinson's Disease. PLoS One 10, e0134087.
Szalardy, L., et al., 2016. Lack of age-related clinical progression in PGC-1alpha-deficient mice - implications for mitochondrial encephalopathies. Behav Brain Res 313, 272–281.
Tanner, C.M., Goldman, S.M., 1996. Epidemiology of Parkinson's disease. Neurol Clin 14, 317–335.
Tsunemi, T., et al., 2012. PGC-1alpha rescues Huntington's disease proteotoxicity by preventing oxidative stress and promoting TFEB function. Sci Transl Med 4 142ra197.
Wang, T., et al., 2016. A Novel Analytical Strategy to Identify Fusion Transcripts between Repetitive Elements and Protein Coding-Exons Using RNA-Seq. PLoS One 11, e0159028.
Weydt, P., et al., 2009. The gene coding for PGC-1alpha modifies age at onset in Huntington's Disease. Mol Neurodegener 4, 3.
Xiao, B., et al., 2017. GWAS-linked PPARGC1A variant in Asian patients with essential tremor. Brain 140, e24.
Ye, Q.Y., et al., 2016. Overexpression of PGC-1 alpha Influences Mitochondrial Signal Transduction of Dopaminergic Neurons. Mol Neurobiol 53, 3756–3770.
Ye, Q., et al., 2017. Mitochondrial Effects of PGC-1alpha Silencing in MPP+ Treated Human SH-SY5Y Neuroblastoma Cells. Front Mol Neurosci 10, 164.
Zhang, Y., et al., 2009. Alternative mRNA splicing produces a novel biologically active short isoform of PGC-1alpha. J Biol Chem 284, 32813–32826.
Zheng, B., et al., 2010. PGC-1alpha, a potential therapeutic target for early intervention in Parkinson's disease. Sci Transl Med *2* 52ra73.
Zheng, L., et al., 2017. Parkin functionally interacts with PGC-1alpha to preserve mitochondria and protect dopaminergic neurons. Hum Mol Genet 26, 582–598.